

Synthesis of Activated Carbon/Chitosan/Alginate Beads Powder as an Adsorbent for Methylene Blue and Methyl Violet 2B Dyes

Margaretha Aditya Kurnia Purnaningtyas, Sri Sudiono, and Dwi Siswanta*

Department of Chemistry, Faculty of Mathematics and Natural Sciences, Universitas Gadjah Mada, Sekip Utara, Yogyakarta 55281, Indonesia

* **Corresponding author:**

tel: +62-274-454188

email: dsiswanta@ugm.ac.id

Received: August 26, 2019

Accepted: January 20, 2020

DOI: 10.22146/ijc.49026

Abstract: The activated carbon-chitosan-alginate (KKA) beads powder was synthesized to form an adsorbent for the cationic dyes, methylene blue (MB) and methyl violet 2B (MV 2B). The aims of this research were to determine the optimum composition of KKA beads powder for the adsorption of cationic dyes and to investigate the effect of pH, adsorbent mass, contact time, and initial concentration of MB and MV 2B dyes. A desorption study was also implemented to predict the adsorption mechanisms of MB and MV 2B dyes. The KKA beads powder was prepared by mixing chitosan, Na-alginate with various variation of masses (0.6; 0.8; 1.0; and 1.2 g) and activated carbon. The KKA beads were immersed in a CaCl₂ solution. The KKA beads powder was characterized using FTIR spectroscopy and SEM. The desorption study was conducted in NaCl (0.1 M and 1.0 M), ethanol (40 and 60%), and pH 4 solution. The result showed that the KKA beads powder had been successfully created, with maximum adsorption capacities of 1.34 mmol g⁻¹ for MB and 1.23 mmol g⁻¹ for MV 2B. The kinetics and isotherms of MB and MV dyes adsorption on the KKA beads powder followed pseudo second order kinetics model and Freundlich isotherm. The desorption study showed that 60% ethanol was the most effective desorption solution for cationic dyes.

Keywords: activated carbon; alginate; chitosan; methylene blue; methyl violet 2B

■ INTRODUCTION

The dyeing process in the textile industry produces 10–15% of the dyes released to the environment [1]. Synthetic dyes have brightness, high color sharpness, and are clearly visible even in very low concentrations [2-3]. MB and MV 2B are cationic synthetic dyes. The presence of synthetic dyes in the environment can disrupt the stability of the organism in the environment due to their carcinogenic, mutagenic, and toxic effects. Therefore, the removal of dyes before being released into the water is very important.

The treatment of dye waste has been carried out by various methods such as biological processes [4], electrochemistry [5], ozonation [6], oxidation [7], photocatalyst [8], membrane filtration [9], and adsorption [10-13]. Adsorption became the most popular and widely used method due to its low operational costs, simple and easy procedure, requires less energy, non-

toxic effects, and because it is highly effective for the degradation of waste [10].

Activated carbon is a porous material that has potential in the removal of chemical species by adsorption [14]. The mesopores and macropores of activated carbon can be used to remove large pollutants such as dyes [15]. According to previous studies, activated carbon is able to adsorb MB [16-18] and MV 2B [3,19]. Modification of activated carbon with biopolymers such as chitosan [12] and alginate [11,13] can also be used as an alternative to remove cationic dyes.

Currently, there is no report about the fabrication of a composite material consisting of activated carbon, chitosan, and alginate to be used as an adsorbent for the removal of cationic dyes. Chitosan and alginate are polycationic and polyanionic natural polymers, respectively. The combination of both polymers will form a polyelectrolyte complex (PEC) due to the

interaction between the carboxyl groups of alginates and the amino groups of chitosan [20]. The formation of PEC enriches the active sites on the surface of the adsorbent.

Therefore, the main objective of this research was to explore the potential of activated carbon-chitosan-alginate (KKA) beads powder as an adsorbent for MB and MV 2B dyes. The aims of the research were to determine the optimum composition of KKA beads powder, to investigate the effect of contact time and initial concentration on the adsorption of MB and MV 2B, and to study the desorption of MB and MV 2B dyes.

■ EXPERIMENTAL SECTION

Materials

Chitosan (%DD c.a. 80%), activated carbon (technical), sodium alginate (MW 120–190 g/mol, G/M = 1.56), and other materials of analytical grade were supplied by Merck including calcium chloride, sodium hydroxide, acetic acid, hydrochloric acid, sodium chloride, ethanol absolute, MB, and MV 2B.

Instrumentation

The equipment used in this research were pH meter (SI Analytics Lab 860), magnetic stirrer, shaker (Memmert), and centrifuge (Thermo Scientific SL 16R). Characterization of the functional groups of the KKA beads powder was detected by Fourier transform infrared spectroscopy (FTIR) (Prestige-21 Shimadzu) at 4000–500 cm^{-1} wavelength. The morphology of the KKA beads powder was characterized by Scanning Electron Microscopy (SEM) (JSM-6510LV). The concentration of dyes was analyzed by Spectrophotometer UV-Vis (Thermoscientific 20D).

Procedure

Synthesis of the activated carbon/chitosan/alginate (KKA) beads powder

Chitosan (1 g) in 30 mL of acetic acid (2.0% v/v) was mixed with sodium alginate (1 g) in 30 mL of acetic acid (2.0% v/v). After the suspension had mixed completely, activated carbon (1 g) was added into the suspension. The suspension of KKA was stirred using a magnetic stirrer for 24 h. Then, the KKA beads were formed by dripping the solution into a CaCl_2 (2.5% b/v) solution. The KKA

beads were washed, dried, and crushed into powder. The same procedure was made for the synthesis of KKA beads powder with mass variations of sodium alginate (0.6; 0.8; and 1.2 g).

The optimum composition of KKA beads powder

The optimum composition of the KKA beads powder was determined by mixing mass variations of sodium alginate (0.6; 0.8; and 1.2 g) during the synthesis of the powder. The resulting KKA beads powder (20 mg) was added into 20 mL of MB or MV 2B dyes solution with concentration of 100 mg L^{-1} and the adsorption was carried out for 60 min. Afterwards, the solid material was separated, and the filtrate was analyzed by spectrophotometry UV-Vis. The adsorption capacity of the adsorbent towards MB and MV 2B dyes were calculated using Eq. (1).

$$\text{Adsorption capacity}(q_t) = \frac{(C_o - C_t)V}{m} \quad (1)$$

where C_o (mg L^{-1}) is the initial concentration of dyes, C_t (mg L^{-1}) is the concentration of dyes after adsorption, m (g) is the mass of the adsorbent, and V (mL) is the volume of the dyes.

Effect of pH

A series of solutions containing 20 mL of 100 mg L^{-1} MB or MV 2B dyes were prepared with pH of 4, 5, 6, 7, 8, and 9. pH adjustment was carried out by adding 0.1 M NaOH and 0.1 M HCl. Into the series of dyes solution, 20 mg of KKA beads powder with optimum composition was added as obtained from the previous experiment. Then the adsorption was carried out for 60 min. The solid material was then separated, and the filtrate was analyzed by spectrophotometry UV-Vis.

Effect of adsorbent dose

The effect of adsorbent dose was investigated by using 10, 20, 30, 40, and 50 mg of KKA beads powder. The varied adsorbent doses were added into 20 mL of 100 mg L^{-1} MB or MV 2B dyes solution. The solution was adjusted to the optimum pH obtained from the previous experiment. Then the adsorption was carried out for 60 min. The solid material was then separated, and the filtrated dyes were analyzed by spectrophotometry UV-Vis.

Effect of contact time

The effect of contact time was determined within the time range of 5–180 min. The optimum adsorbent dose of the KKA beads powder obtained from the previous experiment was added into 20 mL of 100 mg L⁻¹ MB or MV 2B dyes solution at the optimum pH. The adsorption was conducted for 5, 10, 15, 30, 45, 60, 90, 120, 150, and 180 min. The solid material was then separated, and the filtrated dyes were analyzed by spectrophotometry UV-Vis.

Effect of initial concentration

The optimum dose of the KKA beads powder was added into 20 mL of MB or MV 2B dyes solution at optimum pH. The effect of initial concentrations was investigated in 25, 50, 75, 100, 150, 200, 300, 400, 500, 600, 800, and 1000 mg L⁻¹. The adsorption was carried out for the duration of the optimum time as obtained from the previous experiment. The solid material was then separated, and the filtrated dyes were analyzed by spectrophotometry UV-Vis.

Adsorption Selectivity of MB and MV 2B dyes

The adsorption selectivity test between MB and MV 2B dyes was determined in comparison to the mole of MB: MV 2B dyes (1:0, 0:1, and 1:1). The adsorption was investigated in the optimum condition of MB or MV 2B.

Study of desorption

The process of desorption was investigated in NaCl (0.1 and 1.0 M), ethanol (40 and 60%) and pH 4 solution. The time of desorption was carried out for 1, 3, 18, and 24 h. The percentage of desorption was calculated using Eq. (2).

$$\% \text{Desorption} = \frac{C_e}{C_o} \times 100\% \quad (2)$$

where C_e (mg L⁻¹) is the concentration of dyes after desorption and C_o (mg L⁻¹) is the concentration of dyes in the adsorbent.

Isotherm models for the adsorption of MB and MV 2B dyes

The isotherms for the adsorption of MB and MV 2B dyes were determined using two models according to Eq. (3) and (4).

$$\text{Langmuir isotherm: } \frac{C_e}{q_e} = \frac{1}{K_L q_{\max}} + \frac{C_e}{q_{\max}} \quad (3)$$

$$\text{Freundlich isotherm: } \ln q_e = \ln K_F + \frac{1}{n} \ln C_e \quad (4)$$

where K_L (L mg⁻¹) is the Langmuir constant, q_{\max} (mg g⁻¹) represents the monolayer capacity, K_F and n are Freundlich constants, C_e (mg L⁻¹) is the equilibrium concentration, and q_e (mg g⁻¹) is the amount adsorbed at equilibrium.

Kinetics model for the adsorption of MB and MV 2B dyes

The kinetics model for the adsorption of MB and MV 2B dyes was determined using four models according to the following equations:

$$\text{First - order kinetics model: } \ln C_e = \ln C_o - k_1 t \quad (5)$$

$$\text{Second - order kinetics model: } \frac{1}{C_e} = \frac{1}{C_o} + k_2 t \quad (6)$$

$$\text{Pseudo first - order kinetics model: } \ln(q_e - q_t) = \ln q_e - k_1 t \quad (7)$$

$$\text{Pseudo first - order kinetics model: } \frac{t}{q_t} = \frac{1}{k_2 q_e^2} + \frac{t}{q_e} \quad (8)$$

where k (min⁻¹) is the rate constant, t (min) is time, C_o (mg L⁻¹) is the initial concentration, C_e (mg L⁻¹) is the equilibrium concentration, and q_e (mg g⁻¹) is the amount adsorbed at equilibrium.

RESULTS AND DISCUSSION

FTIR Spectra of KKA Beads Powder

FTIR analysis was used to identify several characteristic functional groups of the KKA beads powder. The FTIR spectra of the KKA beads powder before and after the dyes adsorption-desorption are shown in Fig. 1. Fig. 1 shows that activated carbon has characteristic peaks at 1628, 3425, also 2855 and 2924 cm⁻¹ due to stretching vibrations of -C=O, -OH, and -CH. Modified activated carbon peaks shifted from 1628 to 1605 cm⁻¹. This data represented the electrostatic interactions between the -NH₃⁺ of chitosan and -COO⁻ of alginates that form PEC in KKA beads powder. Additional peaks at 1400 and 1034 cm⁻¹ are identical to stretching vibrations of -CH amines from chitosan structures and stretching vibrations of -CO from chitosan and alginate structures.

FTIR spectra after MB and MV 2B dyes adsorption-desorption showed shifting of peaks that occurred due to the interaction between adsorbents and

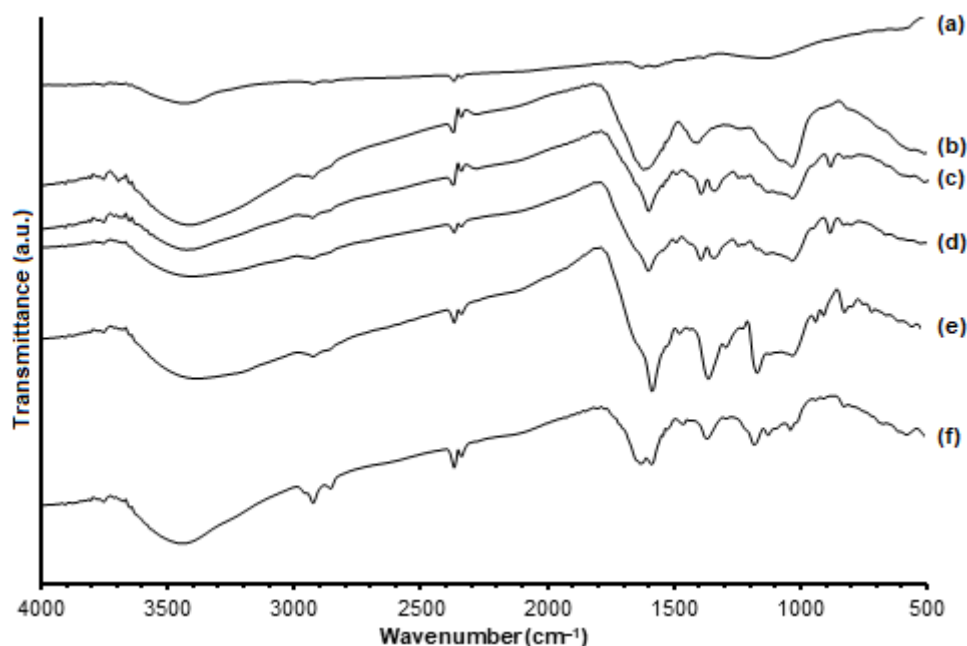


Fig 1. FTIR spectra for (a) activated carbon, (b) KKA beads powder 0.8, KKA beads powder 0.8: (c) after adsorption of MB, (d) after desorption of MB, (e) after adsorption of MV 2B, and (f) after desorption of MV 2B, respectively.

MB/MV 2B dyes [12-13]. After the MB adsorption and desorption, there were new peaks at 1342 and 802 cm^{-1} which show stretching vibrations of $-\text{N}=\text{O}$ and $-\text{CS}$, respectively [18]. The additional peak between 1134 to 1180 cm^{-1} is identical to stretching vibrations of $-\text{CN}$ of the dyes on the surface of the adsorbent [21]. Decreased peak intensity at 1034 cm^{-1} is due to the interaction of dyes and the KKA beads powder [13].

SEM Analysis of KKA Beads Powder

The surface morphology of the KKA beads powder was characterized by SEM analysis. The SEM photograph for activated carbon and the KKA beads powder before and after adsorption-desorption of MB and MV 2B under the same magnifications is given in Fig. 2. Fig. 2 shows that activated carbon has an irregular surface and various pore sizes. The pore size of the KKA

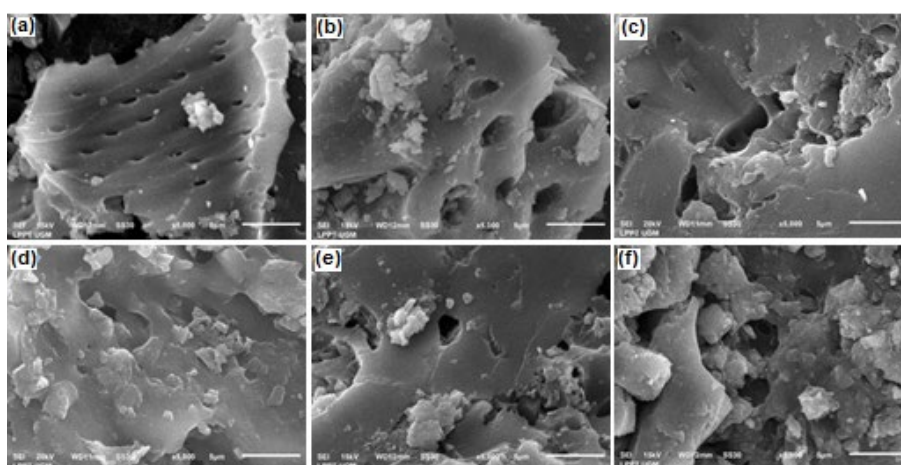


Fig 2. SEM images at 5000 magnifications for – (a) activated carbon, (b) KKA beads powder 0.8, KKA beads powder 0.8: (c) after adsorption of MB, (d) after adsorption of MV 2B, (e) after desorption of MB, and (f) after desorption of MV 2B, respectively

beads powder looks larger than that of the activated carbon. Chemical modification with chitosan and alginate through PEC can increase the pore size of activated carbon, potentially increasing the adsorption capacity of the dyes [13].

According to Fig. 2, the adsorption of dyes caused the surface of the KAA beads powder to be rough with lumps covering the pore of the activated carbon. These lumps indicate the presence of interaction between adsorbent and adsorbate, as well as showing the adsorbates which are trapped in the pores [22]. The SEM image of the KKA beads powder after desorption with 60% ethanol also shows the rough and lumpy surface. It shows that the desorption process is also followed by the removal of the adsorbent material from the surface of the KKA beads powder.

The Optimum Composition of KKA Beads Powder

Fig. 3 shows that the adsorption capacity of dyes decreased as an increasing amount of alginate was added. The formation of the KKA beads was carried out in a solution of CaCl_2 that acted as an agent to form and strengthen the physical properties of the beads. Increasing the amount of alginate increased the $-\text{COO}^-$ group and also increased the risk of the group reacting with Ca^{2+} during the beads formation process. This caused the amount of $-\text{COO}^-$ available to bind with dyes reduced, leading to the decrease of the adsorption capacity. The composition of the KKA beads powder that had maximum adsorption capacity was observed at 0.8 g alginate with $0.284 \text{ mmol g}^{-1}$ (MB) and $0.213 \text{ mmol g}^{-1}$ (MV 2B).

Effect of pH

The effect of pH on the dye adsorption of the KKA beads powder was studied at the pH range of 4–9. The relationship curve between the amount of dyes adsorbed and various pH is shown in Fig. 4. Fig. 4 shows that the dyes adsorption capacity increased along with the increase in pH. The KKA beads powder adsorption capacity tended to decrease after pH 7. The maximum adsorption capacity was observed at pH 7. Therefore, pH 7 was selected as the optimal pH for the dyes removal from aqueous solution using KKA beads powder. The

adsorption capacity of the KKA beads powder at pH 7 was $0.285 \text{ mmol g}^{-1}$ (MB) and $0.216 \text{ mmol g}^{-1}$ (MV 2B).

Chitosan in acidic medium will be protonated to $-\text{NH}_3^+$. The carboxylic group of alginate will maintain its protons thereby reducing the possibility of bonding with other positively charged ions [23]. The presence of an excess amount of free protons in an acidic solution competes with the dyes molecules for adsorption sites on the surface of the adsorbent [24]. At pH close to neutral, the dominant form of chitosan is $-\text{NH}_2$. The presence of $-\text{NH}_2$, $-\text{OH}$, and $-\text{COO}^-$ on the surface of the KKA beads powder can increase interactions with cationic dyes, so the capacity of adsorption increases. Adsorption capacity tends to decrease at basic medium, despite the high availability of $-\text{COO}^-$ on the surface of the adsorbent. This is due to the interaction between OH^- ions and cationic dyes in the solution. [25].

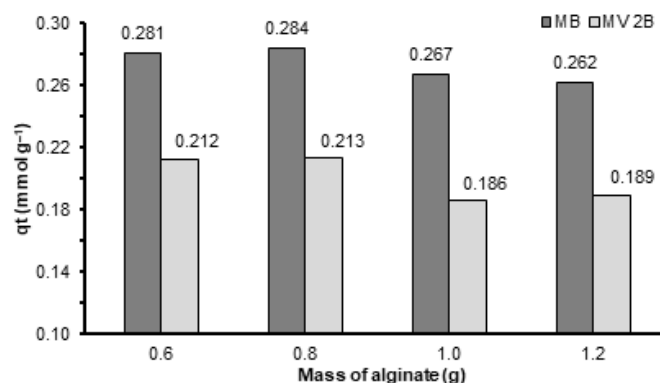


Fig 3. Effect of alginate on MB and MV 2B dyes adsorption onto the KKA beads powder

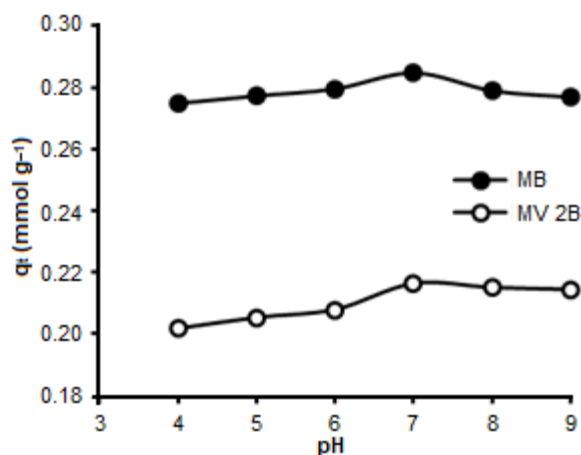


Fig 4. Effect of pH on MB and MV 2B dyes adsorption onto the KKA beads powder

Effect of Adsorbent Dosage

Fig. 5 shows the adsorption capacity and removal percentage of dyes against the adsorbent dosage. The percentage of adsorption increased with increasing amount of adsorbent dosage. As the adsorbent dose increase, the amount of active sites on the surface of the adsorbent also increases, so more dye molecules can adsorb to the surface of the adsorbent. Higher adsorbent dosage however, caused the adsorbent to aggregate reducing the surface area thus decreasing the adsorption capacity [25]. The KKA beads powder optimum dosage in this study was 30 mg with an adsorption percentage of more than 80% for both MB and MV 2B.

Effect of Contact Time

Fig. 6 shows the effect of contact time on the adsorption capacity of the KKA beads powder towards dyes. High adsorption capacity occurs at the beginning of the contact time because the active sites in the adsorbent is still empty, causing the dye molecules to be easily attached to the surface of the adsorbent. The adsorption capacity of the adsorbent towards the MV 2B dye increased gradually with increasing contact time, but the adsorption capacity towards the MB dye decreased after 60 min. The decrease in adsorption capacity is due to the decrease in the number of active sites on the adsorbent.

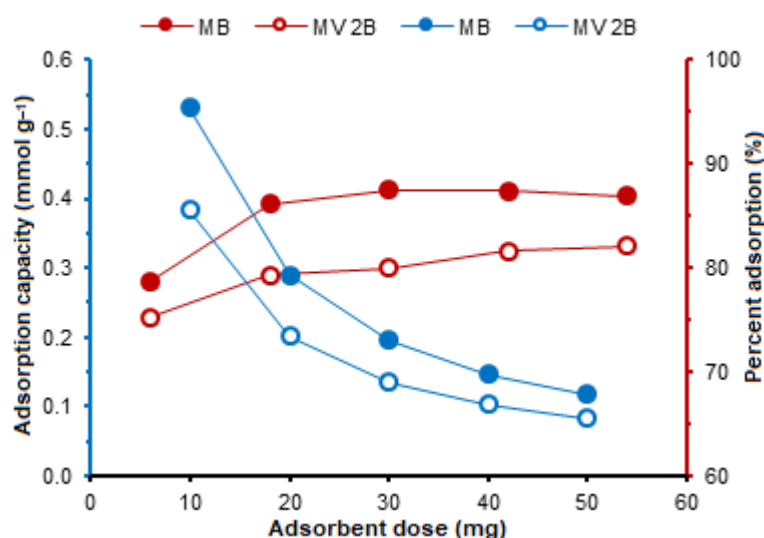


Fig 5. Effect of adsorbent dose of KKA beads powder on adsorption of MB and MV 2B dyes

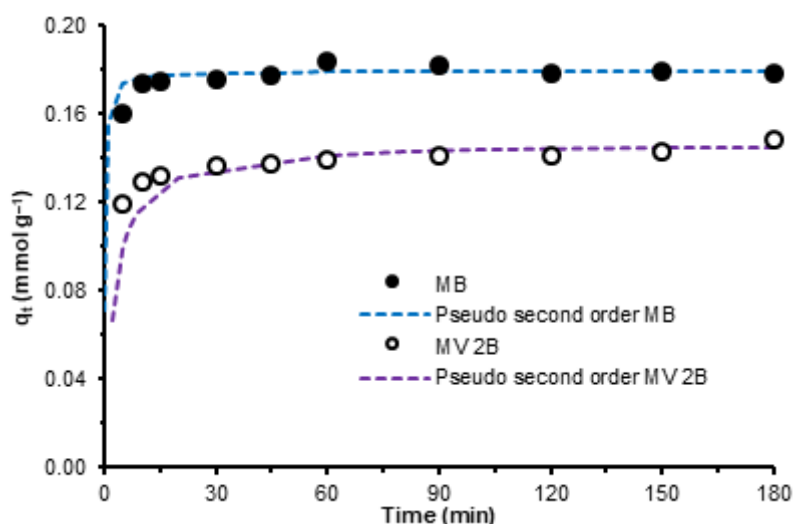


Fig 6. Effect of time on adsorption of MB and MV 2B dyes onto the KKA beads powder

The kinetics model for the KKA beads powder was described using four models, which consisted of the first-order, second-order, pseudo first-order, and pseudo second-order kinetic models. The kinetics data for the KKA beads powder in the various models are shown in Table 1. The R^2 value in the pseudo second-order kinetics model was closer to one, so it can be assumed that the pseudo second-order kinetics model best expressed the adsorption of the KKA beads powder. Theoretically, the pseudo second-order kinetics model describes the adsorption of more than one active sites of the adsorbent.

The dyes had $0.115 \text{ mg g}^{-1} \text{ min}^{-1}$ (MB) and $0.007 \text{ mg g}^{-1} \text{ min}^{-1}$ (MV 2B) of k value. These results illustrate that the adsorption rate of the MB dye was greater than the adsorption rate of MV 2B. Smaller

molecule size are more easily distributed, thus equilibrium would be achieved faster [26]. The MB dye have smaller molecular sizes compared to the MV 2B dye, which explains why higher adsorption rate of MB dye had a larger adsorption rate.

Effect of Initial Concentration

Fig. 7 shows that the adsorption capacity of the dye increased with increasing initial concentration. The adsorption limit which describes the saturation of the adsorbent against the adsorbate is not visible. The chance of the adsorbate interaction with the activated site of the adsorbent will increase with an increasing number of dye molecules in the solution. In this study, the maximum adsorption capacity of the KKA beads was

Table 1. Adsorption kinetics parameters of the adsorption on MB and MV 2B dyes onto the KKA beads powder

Kinetics model	Parameter	MB	MV 2B
	Molecular weight (g mol^{-1})	319.86	393.96
	q_e experiment (mmol g^{-1})	0.183	0.148
First-order	R^2	0.2953	0.8316
	k_1 (min^{-1})	0.001	0.004
Second-order	R^2	0.2845	0.8817
	k_2 (min^{-1})	0.026	0.083
Pseudo first-order	R^2	0.4367	0.9435
	k_1 (min^{-1})	0.007	0.061
	q_e cal (mmol g^{-1})	0.011	0.020
Pseudo second-order	R^2	0.9998	0.9991
	k_2 ($\text{g mmol}^{-1} \text{ min}^{-1}$)	36.8	2.79
	k_2 ($\text{g mg}^{-1} \text{ min}^{-1}$)	0.115	0.007
	q_e cal (mmol g^{-1})	0.179	0.147

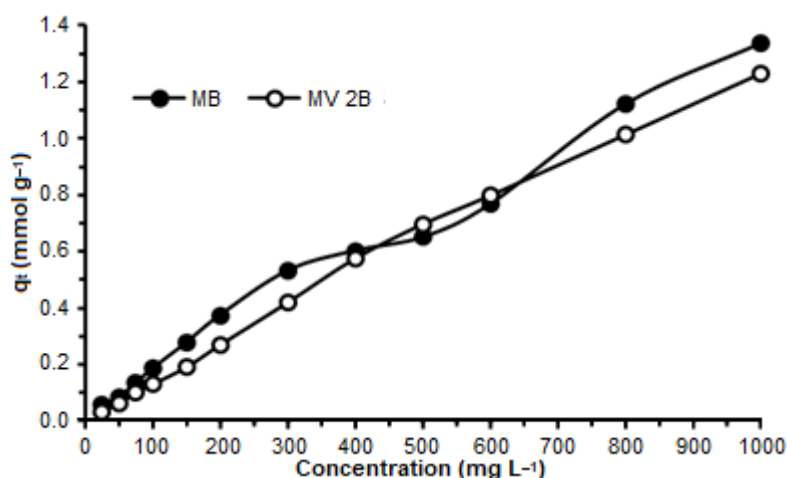


Fig 7. Effect of concentration on adsorption of MB and MV 2B dyes on the KKA beads powder

obtained at 1000 mg L⁻¹, with 1.34 mg g⁻¹ (MB) and 1.23 mg g⁻¹ (MV 2B) adsorption capacity.

The adsorption isotherms studied in this research are Langmuir and Freundlich isotherms. A summary of the adsorption isotherms calculation can be seen in Table 2. Table 2 shows that the R² value in the Freundlich isotherm is closer to one compared to the Langmuir isotherm which means that the MB and MV 2B dye adsorption on the KKA beads powder follow the Freundlich isotherm. Adsorption of MB dyes with zeolite-activated carbon/chitosan beads [12] and activated-alginate beads [13] also followed the Freundlich isotherm. The Freundlich isotherm describes the process of adsorption on heterogeneous surfaces. The heterogeneity factor (1/n) is a characteristic of the Freundlich model. In this study, n values were 1.64 (MB) and 1.16 (MV 2B). The higher n value represents the higher heterogeneity of the

site on the adsorbent.

Selectivity Adsorption of MB and MV 2B Dyes

Fig. 8 shows that the maximum adsorption of dyes are smaller if they are in a multicomponent solution, which proves that there is a competitive effect between the dyes. Under optimum conditions of MB adsorption, the presence of MV 2B reduced MB adsorption by 11.7%. Meanwhile, under the optimum conditions of MV 2B dye adsorption, the presence of MB reduced MV 2B adsorption by 12.3%. These results indicate that the reduction of MV 2B adsorption is greater in multicomponent solutions. In multicomponent solutions, smaller molecules will occupy the pores in the adsorbent structure first [27]. The MB dye have a smaller molecular weight compared to MV 2B causing the molecules of the MB dye to fill the pores of the adsorbent earlier than the MV 2B dye.

Table 2. The Langmuir and Freundlich isotherm parameters for MB and MV 2B dyes

Isotherms model	Parameter	MB	MV 2B
q _e experiment (mmol g ⁻¹)		1.34	1.23
Langmuir isotherm	q _{max} (mmol g ⁻¹)	1.36	2.42
	K _L (L mol ⁻¹)	3135	1552
	E (KJ/mol)	20.1	18.3
	R ²	0.8212	0.8789
Freundlich isotherm	K _F	1.17	2.14
	n	1.64	1.16
	R ²	0.9035	0.9820

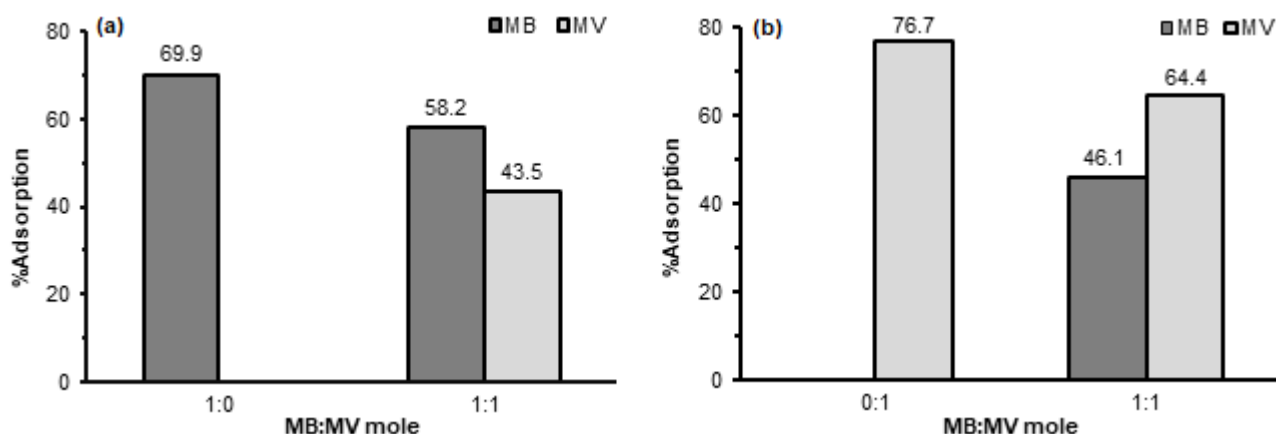


Fig 8. Effect of percentage adsorption of MB and MV 2B dyes under optimum conditions of (a) MB and (b) MV 2B adsorption

MB and MV 2B Dyes Adsorption

Table 3 shows that activated carbon has adsorption capacities of 0.151 mmol g⁻¹ (MB) and 0.171 mmol g⁻¹ (MV 2B) under optimum conditions, while the adsorption capacities of the KKA beads powder are 1.34 mmol g⁻¹ and 1.23 mmol g⁻¹ for MB and MV 2B, respectively. The results showed that the adsorption ability of activated carbon after modification into KKA beads powder increased by 787 and 621% for MB and MV 2B dyes, respectively. The increased adsorption ability of the activated carbon is due to the presence of activated sites on the surface of the adsorbent from chitosan and alginate modification.

Desorption Study

Desorption solution (NaCl) was found to have an influence in the process of releasing cationic dyes -N⁺(CH₃)₂ (MB) and -N⁺HCH₃ (MV 2B) from the adsorbent. The strength of Na⁺ ions was able to release the electrostatic cationic dyes which had been bound to the KKA beads powder. The greater the amount of Na⁺ ions in the solution, the greater amount of MB and MV 2B molecules that was released. pH 4 solution was used as the medium for desorption because it has an acidic strength that can protonate the activated site of chitosan from -NH₂ to -NH₃⁺. Protonated amino groups was able to

increase the hydrophilicity of the adsorbent causing the MB or MV 2B dyes to be released. Ethanol solution in water can also act as a medium of desorption because it can attract MB or MV 2B dyes through hydrogen bonds and hydrophobic interactions [31].

Fig. 9 shows that prolonging the desorption time increased the amount of MB and MV 2B released from the adsorbent. The desorption order for MB and MV 2B dyes were 60% ethanol > pH 4 solution > 40% ethanol > 1.0 M NaCl > 0.1 M NaCl. Therefore, 60% ethanol solution was the most effective desorption medium. This points to the tendency for hydrogen bonds and hydrophobic interactions. The existence of double bonds and benzene rings in the structure of dyes that are hydrophobic gives the possibility that hydrophobic interactions will be more dominant than electrostatic interactions [28].

The percentage of desorption for MB and MV 2B dyes in various solvents were less than 22%. This is likely because only the dye molecules on the surface of the adsorbent were able to be released. The porous structure of the KKA beads powder caused the adsorbed dyes to be trapped and difficult to escape. Similarly, MB desorption studies on carbon monolith (CM) adsorbents using ethanol were only able to adsorb MB dyes attached to the CM surfaces, not in macro and mesoporous adsorbent structures [32].

Table 3. Comparison of MB and MV 2B dye adsorption capacity in various adsorbents

Adsorbent	Dyes	Capacity adsorption		pH	Mass (mg)	Time (min)	Concentration (mg L ⁻¹)	Isotherm model	Reference
		mmol g ⁻¹	mg g ⁻¹						
Activated carbon	MB	0.151	48.2	7	30	60	1000	Freundlich	This work
	MV 2B	0.171	67.2	7	30	180	1000	Freundlich	
KAA beads powder	MB	1.34	428	7	30	60	1000	Freundlich	This work
	MV 2B	1.23	484	7	30	180	1000	Freundlich	
Activated carbon sunflower seed hulls	MV 2B	0.253	92.6	4.5	30	105	300	Freundlich	[3]
Activated carbon-alginate beads	MB	0.719	230	9.5	10	1200	100	Freundlich	[13]
Composite HNT-Fe ₃ O ₄	MV 2B	0.052	20.4	7	15	360	90	Langmuir	[25]
Activated carbon	MB	2.39	742	7	25	1440	3000	Langmuir	[28]
Activated carbon-clay	MB	0.560	179	9	20	1560	400	Langmuir	[29]
Polyglycerol magnetic gel	MB	1.44	459	7	20	120	1600	Langmuir	[30]
	MV 2B	1.01	400	7	20	120	2000	Langmuir	

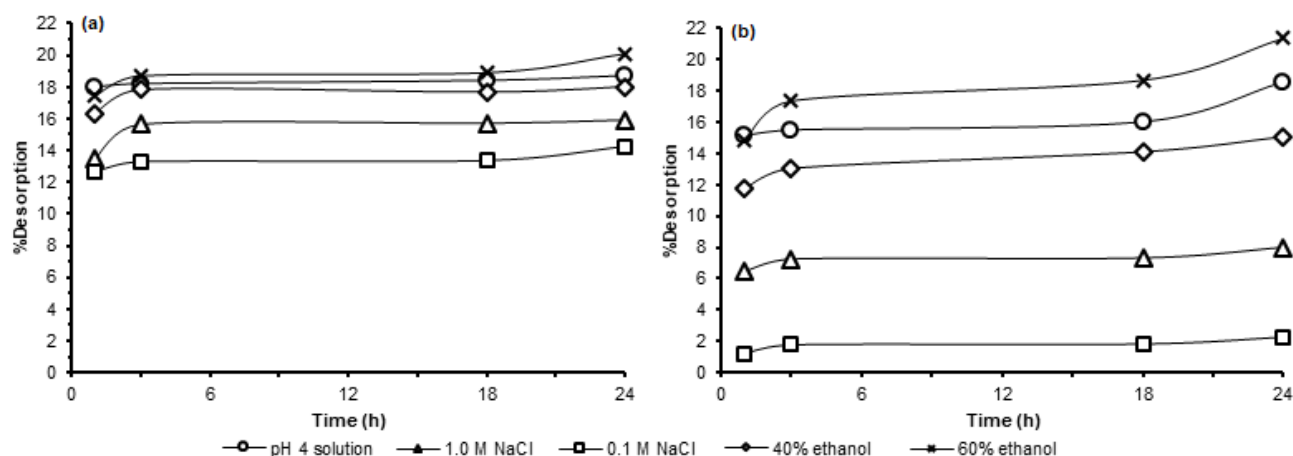


Fig 9. Percentage of desorption for (a) MB and (b) MV 2B dyes

CONCLUSION

The optimum adsorbent composition for adsorption of MB and MV 2B dyes was found in KKA beads powder with 0.8 g of alginate. The optimum contact time was 60 min for the MB dye and 180 min for MV 2B. Both dyes followed a pseudo second-order kinetics model with an adsorption rate of $0.115 \text{ g mg}^{-1} \text{ min}^{-1}$ for MB and $0.007 \text{ g mg}^{-1} \text{ min}^{-1}$ for MV 2B. The optimum initial concentration for both dyes was 1000 mg L^{-1} . Both dyes followed the Freundlich isotherm with K_F and n values of 1.17 and 1.64, respectively for MB, and 2.14 and 1.16 respectively for MV 2B. The most effective desorption medium for MB and MV 2B dyes in the KKA beads powder was 60% ethanol.

ACKNOWLEDGMENTS

This research was financially supported by the Master Thesis Research Program of the Director General of Higher Education, Ministry of Education and Culture, Republic of Indonesia (contract number 2858/UN1.DIT LIT/DIT-LIT/LT/2019).

REFERENCES

- [1] Zhou, L., Huang, J., He, B., Zhang, F., and Li, H., 2014, Peach gum for efficient removal of methylene blue and methyl violet dyes from aqueous solution, *Carbohydr. Polym.*, 101, 574–581.
- [2] Aksu, Z., 2005, Application of biosorption for the removal of organic pollutants: A review, *Process Biochem.*, 40 (3-4), 997–1026.
- [3] Hameed, B.H., 2008, Equilibrium and kinetic studies of methyl violet sorption by agricultural waste, *J. Hazard. Mater.*, 154 (1-3), 204–212.
- [4] Lucas, M.S., Dias, A.A., Sampaio, A., Amaral, C., and Peres, J.A., 2007, Degradation of a textile reactivated Azo dye by a combined chemical-biological process: Fenton's reagent-yeast, *Water Res.*, 41 (5), 1103–1109.
- [5] Orts, F., del Río, A.I., Molina, J., Bonastre, J., and Cases, F., 2018, Electrochemical treatment of real textile wastewater: Trichromy Procion HEXL®, *J. Electroanal. Chem.*, 808, 387–394.
- [6] Al jibouri, A.K.H., Wu, J., and Upreti, S.R., 2015, Continuous ozonation of methylene blue in water, *J. Water Process Eng.*, 8, 142–150.
- [7] Mohod, A.V., Hinge, S.P., Raut, R.S., Bagal, M.V., and Pinjari, D., 2018, Process intensified removal of methyl violet 2B using modified cavity-bubbles oxidation reactor, *J. Environ. Chem. Eng.*, 6 (1), 574–582.
- [8] Liu, H., Zhong, L., Govindaraju, S., and Yun, K., 2019, ZnO rod decorated with Ag nanoparticles for enhanced photocatalytic degradation of methylene blue, *J. Phys. Chem. Solids*, 129, 46–53.
- [9] Zhao, R., Li, Y., Sun, B., Chao, S., Li, X., Wang, C., and Zhu, G., 2019, Highly flexible magnesium silicate nanofibrous membranes for effective removal of methylene blue from aqueous solution, *Chem. Eng. J.*, 359, 1603–1616.

- [10] Rafatullah, M., Sulaiman, O., Hashim, R., and Ahmad, A., 2010, Adsorption of methylene blue on low-cost adsorbents: A review, *J. Hazard. Mater.*, 177 (1-3), 70–80.
- [11] Hassan, A.F., Abdel-Mohsen, A.M., and Fouda, M.M.G., 2014, Comparative study of calcium alginate, activated carbon, and their composite beads on methylene blue adsorption, *Carbohydr. Polym.*, 102, 192–198.
- [12] Khanday, W.A., Asif, M., and Hameed, B.H., 2017, Cross-linked beads of activated oil palm ash zeolite/chitosan composite as a bio-adsorbent for the removal of methylene blue and acid blue 29 dyes, *Int. J. Biol. Macromol.*, 95, 895–902.
- [13] Nasrullah, A., Bhat, A.H., Naeem, A., Isa, M.H., and Danish, M., 2018, High surface area mesoporous activated carbon-alginate beads for efficient removal of methylene blue, *Int. J. Biol. Macromol.*, 107 (Part B), 1792–1799.
- [14] Corcho-Corral, B., Olivares-Marín, M., Fernández-González, C., Gómez-Serrano, V., and Macías-García, A., 2006, Preparation and textural characterisation of activated carbon from vine shoots (*Vitis vinifera*) by H₃PO₄-Chemical activation, *Appl. Surf. Sci.*, 252 (17), 5961–5966.
- [15] Gao, Y., Yue, Q., Xu, S., and Gao, B., 2015, Activated carbons with well-developed mesoporosity prepared by activation with different alkali salts, *Mater. Lett.*, 146, 34–36.
- [16] Hameed, B.H., Din, A.T.M., and Ahmad, A.L., 2007, Adsorption of methylene blue onto bamboo-based activated carbon: Kinetics and equilibrium studies, *J. Hazard. Mater.*, 141 (3), 819–825.
- [17] Li, W., Yue, Q., Tu, P., Ma, Z., Gao, B., Li, J., and Xu, X., 2011, Adsorption characteristics of dyes in columns of activated carbon prepared from paper mill sewage sludge, *Chem. Eng. J.*, 178, 197–203.
- [18] Pathania, D., Sharma, S., and Singh, P., 2017, Removal of methylene blue by adsorption onto activated carbon developed from *Ficus carica* bast, *Arabian J. Chem.*, 10 (Suppl. 1), S1445–S1451.
- [19] Chafidz, A., Astuti, W., Augustia, V., Novira, D.T., and Rofiah, N., 2018, Removal of methyl violet dye via adsorption using activated carbon prepared from *Randu* sawdust (*Ceiba pentandra*), *IOP Conf. Ser.: Earth Environ. Sci.*, 167, 012013.
- [20] Wasupalli, G.K., and Verma, D., 2018, Molecular interactions in self-assembled nano-structures of chitosan-sodium alginate based polyelectrolyte complexes, *Int. J. Biol. Macromol.*, 114, 10–17.
- [21] Xu, R.K., Xiao, S.C., Yuan, J.H., and Zhao, A.Z., 2011, Adsorption of methyl violet from aqueous solutions by the biochars derived from crop residues, *Bioresour. Technol.*, 102 (22), 10293–10298.
- [22] Nitayaphat, W., 2014, Utilization of chitosan/bamboo charcoal composite as reactivated dye adsorbent, *Chiang Mai J. Sci.*, 41 (1), 174–183.
- [23] Vijaya, Y., Popuri, S.R., Boddu, V.M., and Krishnaiah, A., 2008, Modified chitosan and calcium alginate biopolymer sorbents for removal of nickel (II) through adsorption, *Carbohydr. Polym.*, 72 (2), 261–271.
- [24] Li, P., Su, Y.J., Wang, Y., Liu, B., and Sun, L.M., 2010, Bioadsorption of methyl violet from aqueous solution onto Pu-erh tea powder, *J. Hazard. Mater.*, 179 (1-3), 43–48.
- [25] Bonetto, L.R., Ferrarini, F., de Marco, C., Crespo, J.S., Guégan, R., and Giovanela, M., 2015, Removal of methyl violet 2B dye from aqueous solution using a magnetic composite as an adsorbent, *J. Water Process Eng.*, 6, 11–20.
- [26] Chiou, M.S., and Chuang, G.S., 2006, Competitive adsorption of dye metanil yellow and RB15 in acid solutions on chemically cross-linked chitosan beads, *Chemosphere*, 62 (5), 731–740.
- [27] Noroozi, B., and Sorial, G.A., 2013, Applicable models for multi-component adsorption of dyes: A review, *J. Environ. Sci.*, 25 (3), 419–429.
- [28] Iriarte-Velasco, U., Chimeno-Alanís, N., González-Marcos, M.P., and Álvarez-Urriarte, J.I., 2011, Relationship between thermodynamic data and adsorption/desorption performance of acid and basic dyes onto activated carbons, *J. Chem. Eng. Data*, 56 (5), 2100–2109.
- [29] Marrakchi, F., Bouaziz, M., and Hameed, B.H., 2017, Activated carbon–clay composite as an

- effective adsorbent from the spent bleaching sorbent of olive pomace oil: Process optimization and adsorption of acid blue 29 and methylene blue, *Chem. Eng. Res. Des.*, 128, 221–230.
- [30] Song, Y., Duan, Y., and Zhou, L., 2018, Multi-carboxylic magnetic gel from hyperbranched polyglycerol formed by thiol-ene photopolymerization for efficient and selective adsorption of methylene blue and methyl violet dyes, *J. Colloid Interface Sci.*, 529, 139–149.
- [31] Samiey, B., and Ashoori, F., 2012, Adsorptive removal of methylene blue by agar: Effects of NaCl and ethanol, *Chem. Cent. J.*, 6, 14.
- [32] He, X., Male, K.B., Nesterenko, P.N., Brabazon, D., Paull, B., and Luong, J.H.T., 2013, Adsorption and desorption of methylene blue on porous carbon monoliths and nanocrystalline cellulose, *ACS Appl. Mater. Interfaces*, 5, 8796–8804.